Journal of Engineering and Sustainable Development
Vol. 30, No. 03, May 2026
https://jeasd.uomustansiriyah.edu.iq/index.php/jeasd
ISSN 2520-0917
Research Article
https://doi.org/10.31272/jeasd.3384

Behavior of Steel Fiber Reinforced Concrete Deep Beams at Elevated Temperature

Jawad K. Al-Bayati[1*], Mohammed Hashim Mohammed[2], Esraa Kh. Mohsin Abuzaid[3], Siti A. Osman[4]

[1,2,3] Highway and Transportation Engineering Department, College of Engineering, Mustansiriyah University, Baghdad, Iraq
[3,4] Department of Civil Engineering, Faculty of Engineering & Built Environment, Universiti Kebangsaan Malaysia (UKM), Selangor, Malaysia.

[*]Email: dr.jawad_albayati@uomustansiriyah.edu.iq

Article Info

Received 14/04/2025
Revised 14/04/2026
Accepted 18/04/2026

Abstract

This paper presents an experimental investigation on the behavior of steel fiber reinforced concrete deep beams at elevated temperature. Twelve reinforced concrete deep beams were cast and tested. The beams were tested under a four-point loading scheme after being subjected to elevated temperatures of 25 (room temperature), 200 °C, and 400 °C. Three volumetric steel fiber ratios of 0, 0.2 and 0.4% and two ratios of shear span to effective depth of 0.4 and 0.8, were used. Results show that ultimate loads of deep beams are increased when heated at 200°C by 69.39%, 28.75% and 4.24%, and decreased when heated at 400°C by 2.04%, 25%, and 42.37% for steel fiber ratios of 0, 0.2%, and 0.4%, respectively. Steel fibers perform better in unheated beams. Incorporating 0.2 and 0.4% of steel fibers increases ultimate loads by 63.27% and 140.82% for unheated beams, 24.1% and 48.19% for beams heated at 200°C, and 25% and 41.67% for beams heated at 400°C, respectively. Also, the shear span to effective depth ratio still dominates the strength of deep beams at elevated temperature as at ambient temperature.

Keywords: Deep Beams, Elevated Temperature, Reinforced Concrete, Shear Behavior, Steel Fiber.

1. Introduction

A deep beam can be defined as a member whose depth is comparable to its span with a relatively small third dimension (width), so it is loaded primarily in its plane. [1], [2]. ACI 318-19 [3] specifies that a beam is considered deep if the ratio of its clear span to depth or shear span to depth does not exceed 4 and 2, respectively. Clear span to depth ratio is limited to less than 3 in Eurocode 2 [4] for a beam to be deep. However, deep beams are characterized by the fact that the majority of the load is directly transmitted from loading points to supports by an arch action through compression struts within shear spans [5]-[8].

Deep beams have many structural applications in bridges, tall buildings, marine structures, foundations, and diaphragms [8]-[9]. Unlike slender beams, shear deformation in deep beams is significant and cannot be neglected, where shear strength rather than flexural strength is the main concern in deep beam design to avoid brittle shear failure [10]-[13].

Many studies have shown that the shear strength and behavior of reinforced concrete deep beams depend primarily on the shear span-to-depth ratio, concrete strength, and flexural and shear reinforcement. Shear capacity increases as the shear span-to-depth ratio decreases or as concrete strength and reinforcement increase [12], [14], [15]. Depending on these parameters, deep beams mainly fail by diagonal splitting, strut crushing, shear-compression, anchorage, or bearing [1], [2], [15]-[17].

The shear behavior of deep concrete beams reinforced with glass fiber reinforced polymer bars for flexure and those without shear reinforcement was examined by Abed et al. [18]. According to the findings, beams reinforced with fiber-reinforced polymer bars exhibited greater deformation and reduced stiffness at their maximum failure load, followed by abrupt failure. Farghaly and Benmokrane [19] discovered that while the type of fiber reinforcement had no bearing on the behavior of the tested beams, the ultimate capacity and deflection characteristics of deep beams longitudinally reinforced by carbon and glass fiber reinforced polymer bars without shear reinforcement were clearly influenced by the reinforcement ratio and concrete compressive strength.

Abed et al. [20] showed that the presence of basalt microfibers in short beams reinforced longitudinally with Basalt Fiber Reinforced Polymer (BFRP) bars increased shear strength by 42% and enhanced overall stiffness and toughness. Kachouh et al. [21] studied the shear response of recycled aggregate concrete deep beams with circular openings using steel fibers as a replacement for the conventional shear reinforcement. The addition of steel fibers remarkably improved the shear response of the tested beams by 39 to 84%. The use of 1% steel fiber without stirrups restores 96% of the original shear capacity of the beam with conventional steel stirrups.

Cycles of heating-cooling frequently occur in concrete structures, either routinely, like in furnaces, chimneys, and power plants, or accidentally when subjected to fire, then water extinguishers [22], [23]. Elevated temperatures have harmful effects and can result in severe damage to concrete, including reductions in strength and stiffness, high permanent deformations, and brittle failure. These effects can be attributed to the changes in the morphology of concrete at high temperatures [5], [22], [24], [25].

Previous research revealed that brittle shear failure is common in reinforced concrete beams subjected to elevated temperatures [5]. It has been demonstrated that the use of steel fibers improves flexural, shear, and ductility performance by bridging cracks and reducing their widths, resulting in internal stress redistribution, thereby preventing this abrupt failure in both deep and slender concrete beams, particularly at elevated temperatures [12], [25], [26]. Moreover, steel fibers can serve as mass reinforcement, which arrests crack propagation by transferring tensile stresses across crack surfaces, leading to enhanced shear response to be more ductile and reduce or even eliminate the conventional shear reinforcement [27]. However, the improvement of using steel fibers is negatively affected by high temperatures, which reduce the bond with the concrete matrix [28].

From the reviewed literature, a critical gap exists in understanding the combined effects of steel fibers and heat on the structural behavior of deep beams, so this study aims to experimentally investigate this behavior and load-carrying capacity, shear performance, and crack patterns.

The novelty of this study lies in providing a comprehensive experimental dataset on the residual shear behavior of steel fiber-reinforced concrete deep beams, a critical structural element often left uninvestigated in fire-resistance research. This research provides new insights into how steel fibers bridge cracks and restrains explosive spalling in deep beams under shear-critical conditions. The findings contribute to the development of design guidelines for fire-resistant, high-strength steel fiber-reinforced concrete deep beams and validate the efficacy of steel fibers in mitigating strength loss in high-stress, high-temperature scenarios.

2. Methods and Materials

To accomplish the aim of the present work, twelve reinforced concrete deep beams were cast and tested. The beams were tested under a four-point loading scheme after being subjected to elevated temperatures of 25 (room temperature), 200 °C, and 400 °C. Three volumetric steel fiber ratios of 0, 0.2 and 0.4% and two ratios of shear span to effective depth (a/d) of 0.4 and 0.8, were used in the tested deep beams. Details of the experimental procedure are presented in the following sections.

2.1. Materials

The materials used in this investigation are:

1. Ordinary Portland cement satisfying Iraqi standard specification No.5-1984 [29].
2. Coarse aggregate (crushed gravel) with a nominal maximum size of 10 and fine aggregate (sand), satisfying Iraqi Standard Specification No.45-1984 [30].
3. Tap water for aggregate washing, concrete mixing, and curing of specimens.
4. Steel reinforcement: φ10 mm with a yield strength of 530 MPa and φ3 mm with a yield strength of 428 MPa used for all beams.
5. Steel fibers: straight steel fibers with aspect ratio (L/d) of 65 (length = 13mm and diameter = 0.2mm) and yield stress of 1130 MPa (from manufacturer's data). The used steel fibers are shown in Fig. 1.

Figure 1. Used steel fibers.

2.2. Concrete Mix Proportions

Mix proportions of the used concrete are 320 kg/m^3 for cement, 640 kg/m^3 for fine aggregate, and 1280 kg/m^3 for coarse aggregate. The water/cement ratio was 0.5 for all mixes. Three mixes were used in the deep beams with steel fiber ratios of 0, 0.2, and 0.4%. The compressive and splitting tensile strengths were determined by testing concrete cubes and cylinders at 28 days according to BS EN 12390-3:2019 [31] and ASTM C496-11 [32], respectively, as shown in Fig. 2 and listed in Table 1.

(a)

(b)

Figure 2. Testing of (a) compressive strength and (b) splitting tensile strength.

Table 1. Compressive and splitting tensile strengths of Concrete Mixes.

Steel fiber ratio, %	Cube Compressive strength, MPa	Splitting tensile strength, MPa
0	30.71	3.11
0.2	34.82	3.69
0.4	37.20	4.12

2.3. Mixing and Casting

Concrete was mixed using a horizontal rotary mixer in a traditional manner, initially mixing sand and coarse material for almost two minutes. After that, cement was added, and the dry elements were combined for three minutes to create a uniform dry mixture. After that, water was added, and the mixture was mixed while the steel fibers were gradually added until it was homogenous. Every aggregate, both fine and coarse, was utilized in a dry, saturated surface condition.

Steel reinforcements were inserted into the molds after they had been cleaned, their inside surfaces oiled, and pieces fastened. The particular concrete was continually poured into molds to create deep beams, which were then compacted using a vibrating table.

Three cubes (100mm×100mm×100mm) and three cylinders (100mm×200mm) were cast with each mix to determine compressive and splitting tensile strengths, respectively. After 24 hours, all specimens were demolded and cured in water for 28 days.

2.4. Details of Deep Beams

Twelve reinforced concrete deep beams of dimensions (600mm×280mm×70mm) were tested under a four-point loading scheme in this work. Three variables are adopted in the tested beams: temperature (T = 25, 200, and 400 °C), steel fiber ratio (SF = 0, 0.2, and 0.4%), and shear span to effective depth ratio (a/d = 0.4 and 0.8). Each deep beam is designated using the letter B (beam) followed by three characters for SF, T, and a/d, respectively, as illustrated in Fig. 3. For example, the beam B4-R-8 is a deep beam that contains 0.4% steel fiber, heated at 25 °C, and tested with a/d of 0.8.

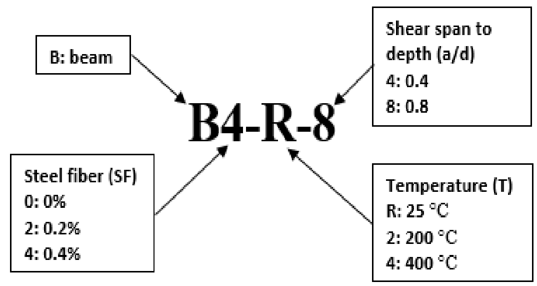

Figure 3. Designation of the deep beams.

Longitudinal and transverse reinforcement were kept the same (2Ø10mm bottom, 2Ø3mm top, and stirrups Ø3mm at 80mm, respectively) as shown in Fig. 4.

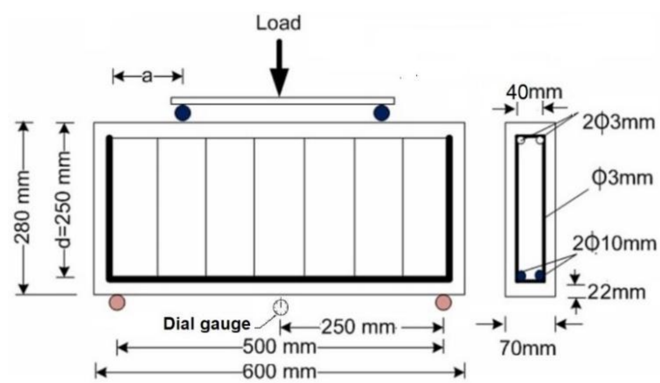

Figure 4. Details and set-up of the tested beam.

2.5. Heating and Testing Procedure

Deep beams were heated using a laboratory electrical furnace with internal dimensions of 750 mm x 600 mm x 500 mm at a slow rate of heating (2°C /min). When the required temperature was reached, it was kept at that level for two hours, then the furnace was turned off, and natural cooling started for about 24 hours before being removed from the furnace and prepared for testing. It is worth noting that the recorded temperature is the reading of the furnace.

A universal testing machine with a 3000 kN capacity was used to test all beams over a simply supported span of 500 mm, as illustrated in Fig. 5, under monotonically increasing static loads in tiny increments until failure. A mechanical dial gauge with a 0.01 mm precision mounted to the bottom side of the beam was used to measure the vertical mid-span deflection (in 5 kN intervals). Throughout the test, crack growth and propagation were tracked and noted. The tested beams' failure modes were also observed.

(a) (b)

Figure 5. (a) Testing machine, (b) a beam under testing.

3. Results and Discussion

3.1. General Response, Cracking Behavior, and Failure of Deep Beams

The structural behavior of all tested deep beams is generally similar, where at first, no visible deformation or cracks appear. With further loading, flexural cracks initiated on the bottom side at or near the middle region between the loading points within approximately 40-50% of the ultimate load. These cracks were generally few and hairy and did not extend upward more than about 50-60% of the beam depth. This observation was also reported by [1].

Afterward, a diagonal crack developed at one or both shear spans. With increasing load, diagonal cracks widened and propagated upward to the loading points and downward to the supports. Eventually, the width of diagonal cracks increased, bearing cracks suddenly formed at supports and propagated upward, accompanied by concrete crushing due to excessive loading and stress concentration, and the beam failed. Deep beams with a lower a/d (0.4) show more ductile failure (especially fibrous ones) than those with a/d of 0.8. Fig. 6 shows the tested deep beams after failure

The load-deflection behavior of the tested deep beams was initially lower, then showed lower stiffness up to failure, where the curve slightly flattened in some beams, as shown in Fig. 7. This response is attributed to the fact that shear governs the behavior of deep beams rather than flexure, where shear failure occurs before yielding of flexural reinforcement, especially for low values of a/d. Other researchers observed similar behavior. [1], [33].

Lower initial stiffness is observed in beams B0-4-4 and B0-4-8 as a result of being non-fibrous and heated at 400°C, as compared to other fibrous beams or beams heated at lower temperatures. More detailed discussions regarding load-deflection behavior and the factors affecting it are presented in the next sections.

3.2. Effect of Elevated Temperature

The effect of elevated temperature on the behavior of the tested deep beams is illustrated in Table 2 and Figs. 8 to 11. As shown in Table 2 and Fig. 8, a relative residual load is the post heated (residual) load value expressed as a percentage of the respective preheated (original) load value.

$$Relative\ residual\ load = \frac{Residual\ load}{Original\ load} \times 100\% \qquad (1)$$

The beams at 200°C are higher than those for unheated beams. Increasing ratios are 169%, 129%, and 104% for steel fiber ratios of 0, 0.2%, and 0.4%, respectively. The increase in strength typically occurs within the temperature range of 150–350°C [34], [35]. This increase can be attributed to the rapid evaporation of free water from both the pore structure and cement gel, which enhances interparticle surface attraction within the cement matrix. This, in turn, results in a denser microstructure and stiffer mechanical behavior under compressive stresses, contributing to the observed strength gain. At 400°C, residual load ratios were 98%, 75%, and 58% for steel fiber ratios of 0, 0.2%, and 0.4%, respectively, as compared to unheated beams. This reduction may be because of losing water and breaking the bond from the cement paste as a result of the decomposition of calcium hydroxide [36].

It can be seen from the above results that as the steel fiber ratio increases from 0 to 0.4%, the deterioration in flexural strength of the tested deep beams at an elevated temperature of 400°C becomes higher (42.37% reduction). In contrast, the strength gain at 200°C becomes lower (only 4.24% increasing). This behavior is due to the fact that steel fibers are used mainly to enhance the tensile strength of concrete by arresting cracks in cement paste, and when the temperature increases, the bond between fibers and cement paste (then their bridging effect) diminishes and results in weaker concrete [28]. This weakness due to elevated temperature becomes more effective when the steel fiber ratio increases.

B0-R-8

B0-2-8

B0-4-8

B2-R-8

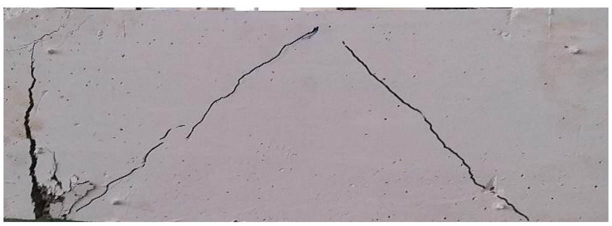

B2-2-8

B2-4-8

B4-R-8

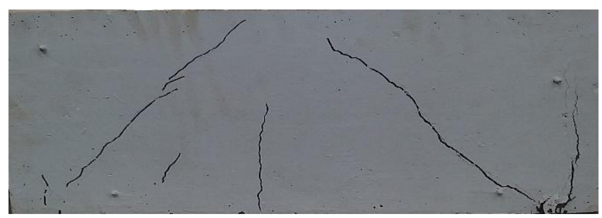

B4-2-8

B4-4-8

B0-4-4

B2-4-4

B4-4-4

Figure 6. Deep beams after failure.

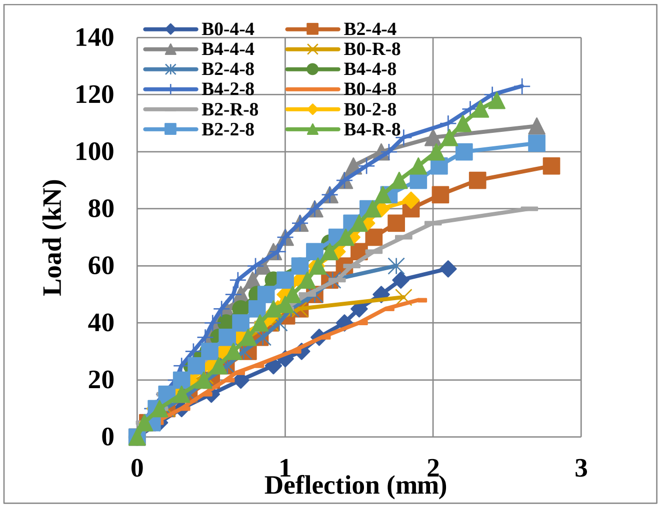

Figure 7. Load-deflection curves of all deep beams.

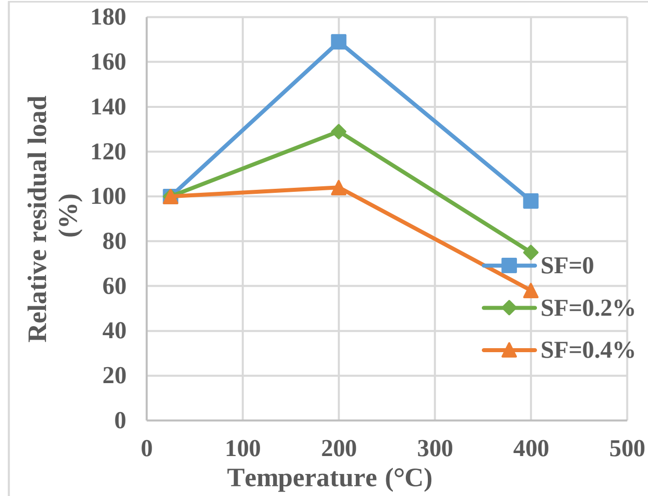

Figure 8. Effect of elevated temperature on relative residual load with a/d =0.8.

Table 2. Effect of elevated temperature on deep beams results.

Beam	Elevated Temperature (T), ° C	Steel Fiber (SF), %	Shear span/effective depth (a/d)	Ultimate Load (kN)	relative residual load (%)	Difference ratio (%)	Maximum Deflection (mm)
B0-R-8	25	0	0.8	49	100	0.00	1.8
B0-2-8	200	0	0.8	83	169	+69.39	1.85
B0-4-8	400	0	0.8	48	98	-2.04	1.9
B2-R-8	25	0.2	0.8	80	100	0.00	2.65
B2-2-8	200	0.2	0.8	103		+28.75	2.7
B2-4-8	400	0.2	0.8	60	75	-25.00	1.75
B4-R-8	25	0.4	0.8	118	100	0.00	2.43
B4-2-8	200	0.4	0.8	123	104	+4.24	2.6
B4-4-8	400	0.4	0.8	68	58	-42.37	1.3

Load-deflection behavior of deep beams under elevated temperature is shown in Figs. 9 to 11 for different steel fiber ratios. Generally, as compared to unheated beams, beams heated at 200°C show stiffer behavior (lower deflections) and higher energy absorption (toughness or area under the curve), while higher deflections and lower energy absorption are exhibited by beams heated at 400°C. However, beam B4-4-8 with 0.4% steel fiber shows lower deflections at 400°C than the corresponding unheated beam B4-R-8 (Fig. 11) but still shows brittle failure at lower ultimate load.

Maximum deflections range from 1.3mm to 2.7mm, with generally higher values for beams heated to 200°C and higher ultimate loads, which exhibit ductile response and can sustain more deformation before failure.

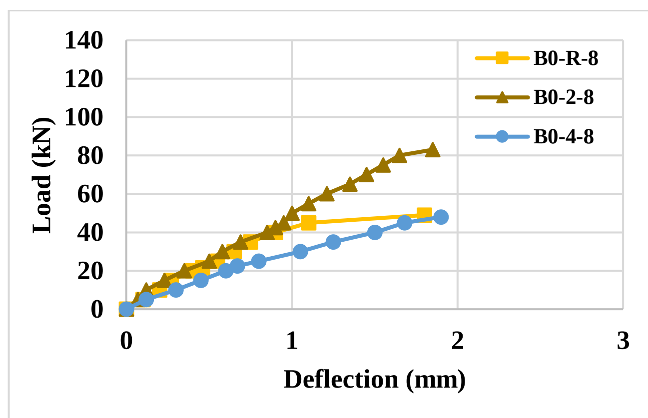

Figure 9. Load-deflection curves of deep beams with SF = 0% and a/d = 0.8.

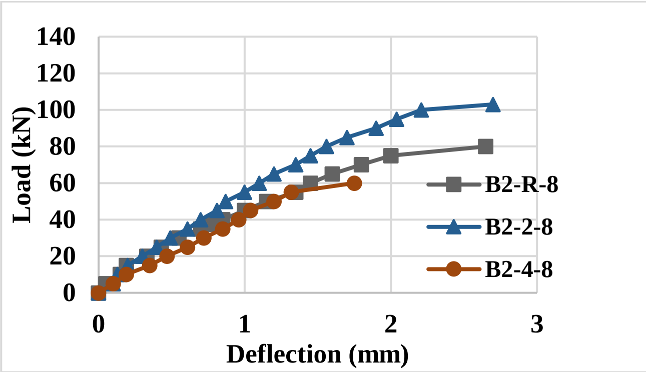

Figure 10. Load-deflection curves of deep beams with SF = 0.2% and a/d = 0.8.

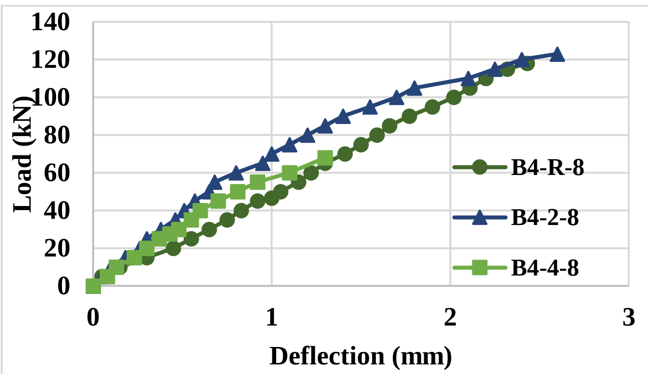

Figure 11. Load-deflection curves of deep beams with SF = 0.4% and a/d = 0.8.

3.3. Effect of Steel Fibers

The effect of the volumetric ratio of steel fibers on the behavior of the tested deep beams is illustrated in Table 3 and Figs. 12 to 15. As shown in Table 3 and Fig. 12, the ultimate loads of beams increase when the steel fiber ratio increases from 0 to 0.2% and 0.4%. Increasing ratios are 63.27% and 140.82% for unheated beams, 24.1% and 48.19% for beams heated at 200°C, and 25% and 41.67% for beams heated at 400°C, respectively. This increase is expected as a result of the increased tensile strength of concrete by incorporating steel fibers, which delays the formation and propagation of diagonal cracks and failure.

The above results indicate that steel fibers perform better in unheated beams (higher increasing ratios) than heated beams due to the negative effect of elevated temperature on steel fiber performance as mentioned earlier (section 3.2). However, decreasing the shear span to effective depth ratio (a/d) from 0.8 to 0.4 makes steel fibers more effective for beams heated at 400°C (increasing ratios of 61.02% and 84.75% for steel fiber ratios of 0.2% and 0.4%, respectively) as shown in Table 3.

The load-deflection behavior of plain and fibrous deep beams is shown in Figs. 13 to 15 for heated and unheated beams. Generally, stiffer behavior (lower deflections) and higher energy absorption can be noticed as the steel fiber ratio rises from 0 to 0.4%.

Maximum deflections of fibrous beams are generally higher than plain ones and range from 1.3mm to 2.8mm. However, Fig. 15 shows that fibrous beams heated at 400°C have lower maximum deflections than plain beams because of the early brittle failure of beams under elevated temperature.

Table 3. Effect of steel fiber on deep beams results.

Beam	Steel Fiber (SF), %	Elevated Temperature (T), ° C	Shear span/effective depth (a/d)	Ultimate Load (kN)	Increasing ratio (%)	Maximum Deflection (mm)
B0-R-8	0	25	0.8	49	0.00	1.8
B2-R-8	0.2	25	0.8	80	63.27	2.65
B4-R-8	0.4	25	0.8	118	140.82	2.43
B0-2-8	0	200	0.8	83	0.00	1.85
B2-2-8	0.2	200	0.8	103	24.10	2.7
B4-2-8	0.4	200	0.8	123	48.19	2.6
B0-4-8	0	400	0.8	48	0.00	1.9
B2-4-8	0.2	400	0.8	60	25.00	1.75
B4-4-8	0.4	400	0.8	68	41.67	1.3
B0-4-4	0	400	0.4	59	0.00	2.1
B2-4-4	0.2	400	0.4	95	61.02	2.8
B4-4-4	0.4	400	0.4	109	84.75	2.7

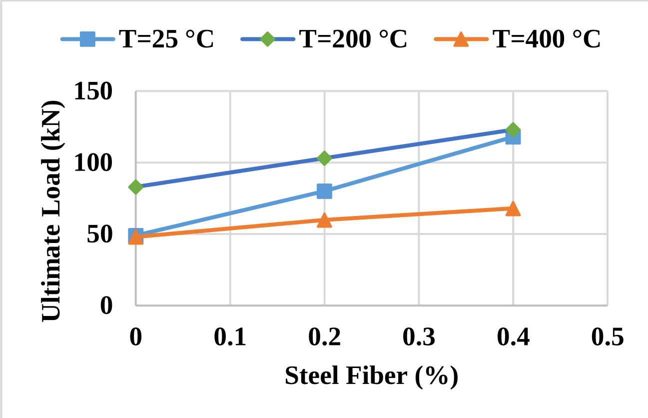

Figure 12. Effect of steel fiber ratio on ultimate loads. with a/d =0.8.

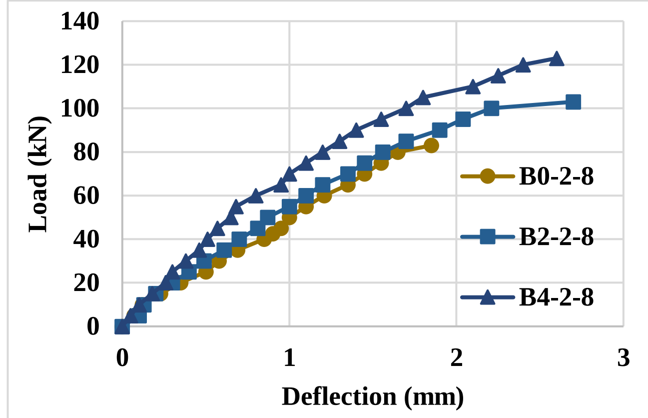

Figure 14. Load-deflection curves of deep beams with T = 200 °C and a/d = 0.8.

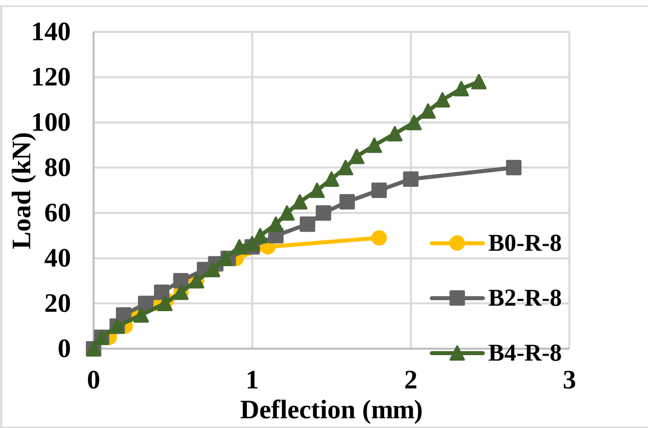

Figure 13. Load-deflection curves of deep beams with T = 25 °C and a/d = 0.8.

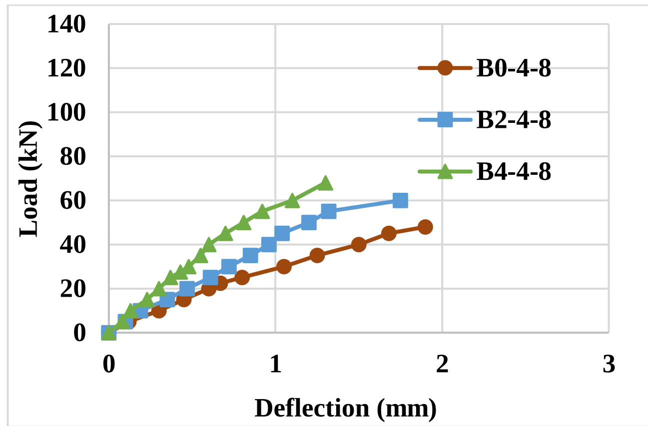

Figure 15. Load-deflection curves of deep beams with T = 400 °C and a/d = 0.8.

.

3.4. Effect of Shear Span to Effective Depth Ratio

The effect of the shear span to effective depth ratio (a/d) on the behavior of the tested deep beams is illustrated in Table 4 and Figs. 16 and 17. As shown in Table 4 and Fig. 16, the ultimate loads of beams under an elevated temperature of 400 °C increase when a/d decreases from 0.8 to 0.4. Increasing ratios are 22.92%, 58.33%, and 60.29% for beams with steel fiber ratios of 0, 0.2%, and 0.4%, respectively. Again, results show that the addition of steel fibers doubles the positive effect of reducing a/d. These results show that even at elevated temperature, shear span to effective depth ratio still has impact on strength of deep beams as at ambient temperature that mentioned in the literature.

Fig. 17 shows that in addition to increasing ultimate loads, decreasing a/d for beams heated at 400 °C from 0.8 to 0.4 causes a tougher and more ductile load-deflection response with higher maximum deflections (2.1-2.8mm) as compared to (1.3-1.9mm) for beams with a/d of 0.8.

Table 4. Effect of shear span to effective depth ratio on deep beams results.

Beam	Shear span/effective depth (a/d)	Steel Fiber (SF), %	Elevated Temperature (T), ° C	Ultimate Load (kN)	Increasing ratio (%)	Maximum Deflection (mm)
B0-4-8	0.8	0	400	48	0.00	1.9
B0-4-4	0.4	0	400	59	22.92	2.1
B2-4-8	0.8	0.2	400	60	0.00	1.75
B2-4-4	0.4	0.2	400	95	58.33	2.8
B4-4-8	0.8	0.4	400	68	0.00	1.3
B4-4-4	0.4	0.4	400	109	60.29	2.7

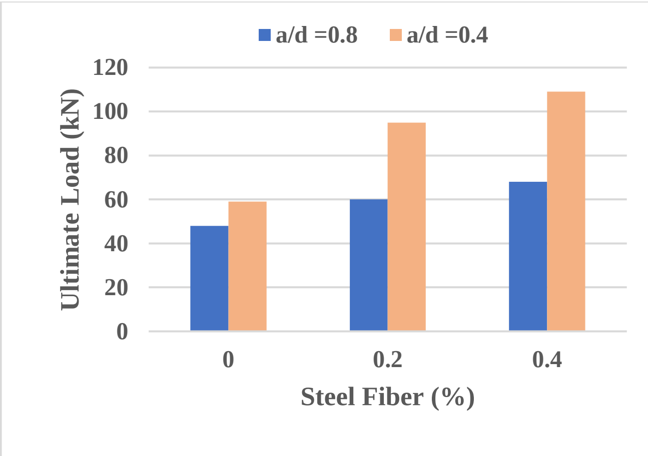

Figure 16. Effect of shear span to effective depth ratio on ultimate loads at temperature =400 °C.

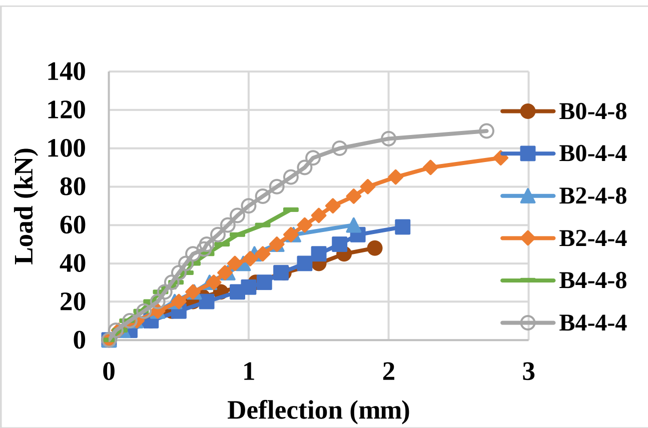

Figure 17. Load-deflection curves of deep beams with T = 400 °C and a/d = 0.4 or 0.8.

4. Conclusions

From the results of the experimental investigation conducted in this work on deep beams, the following conclusions can be drawn. The structural behavior of all tested deep beams is generally similar regarding deformation, cracking, and failure. The load-deflection behavior was initially lower, then showed lower stiffness up to failure, which was characterized by diagonal cracking followed by bearing cracking at supports. Ultimate loads of deep beams heated at 200°C are higher than those of beams at ambient temperature by 69.39%, 28.75%, and 4.24% for steel fiber ratios of 0, 0.2%, and 0.4%, respectively. This increase may be due to further accelerated hydration of cement under higher temperatures. At 400°C, ultimate loads decrease by 2.04%, 25%, and 42.37% for steel fiber ratios of 0, 0.2%, and 0.4%, respectively, as compared to unheated beams. Incorporating 0.2 and 0.4% of steel fibers increases ultimate loads by 63.27% and 140.82% for beams at ambient temperature, 24.1% and 48.19% for beams heated at 200°C, and 25% and 41.67% for beams heated at 400°C, respectively. This indicates that steel fibers perform better for beams at ambient temperature (higher increasing ratios) than heated beams due to the negative effect of elevated temperature on the steel fiber bond with the cement matrix.

Shear span to effective depth ratio still dominates the strength of deep beams at elevated temperature as at ambient temperature. Ultimate loads of beams under elevated temperature of 400 °C increase when a/d decreases from 0.8 to 0.4 by 22.92%, 58.33%, and 60.29% for beams with steel fiber ratios of 0, 0.2%, and 0.4%, respectively. Load-deflection curves of deep beams show higher stiffness, higher energy absorption, and lower deformation when temperature increases from 25 to 200 °C, steel fiber ratio increases from 0 to 0.2 and 0.4%, or shear span to effective depth ratio decreases from 0.8 to 0.4. Brittle behavior is observed for deep beams heated at 400 °C as compared to 25 and 200°C

Competing Interests

The authors declare there are no competing interests.

Author Contribution

Jawad K. Al-Bayati: proposed the research problem. All authors conducted the work equally.

Acknowledgments

The authors would like to reveal their appreciation and gratitude to the respected reviewers and editors for their constructive comments.

Conflict of interests

The authors have no competing interests to declare that are relevant to the content of this article.

References

[1] K. S. Ismail, “Shear Behavior of Reinforced Concrete Deep Beams,” Ph.D. dissertation, University of Sheffield, Sheffield, U.K., 2016.

[2] Reinforced Concrete Deep Beams, Boca Raton, FL, USA: CRC Press, 1991.

[3] ACI 318-19, “Building Code Requirements for Structural Concrete,” Farmington Hills, MI, USA: American Concrete Institute, 2019.

[4] EN 1992-1-1:2004, “Design of Concrete Structures—Part 1-1: General Rules and Rules for Buildings,” Brussels, Belgium: British Standards Institution, 2004.

[5] A. S. Alqarni, A. S. Albidah, and A. A. Abadel, “Shear performance of reinforced concrete deep beams using different coarse aggregates under the effect of elevated temperatures,” Case Studies in Construction Materials, vol. 16, p. e01087, 2022. doi: https://doi.org/10.1016/j.cscm.2022.e01087.

[6] Q. M. Shakir and A. F. Alghazali, “Effect of the arching action on the behavior of the RC precast concrete deep beams: Comparison between several hybrid models,” Journal of Building Rehabilitation, vol. 9, p. 23, 2024. doi: https://doi.org/10.1007/s41024-023-00377-0.

[7] F. Cakir and M. A. Ozdemir, "Strut-and-tie modeling of intraply hybrid composite-strengthened deep RC beams," Buildings, vol. 15, no. 21, p. 3810, 2025. doi: https://doi.org/10.3390/buildings15213810.

[8] R. Tuchscherer, D. Birrcher, M. Huizinga, and O. Bayrak, "Distribution of stirrups across web of deep beams," ACI Structural Journal, vol. 108, no. 1, pp. 108–115, 2011. doi: https://doi.org/10.14359/51664208.

[9] H. Mirzaaghabeik, N. S. Mashaan, and S. K. Shukla, "Shear behavior of ultra-high-performance concrete deep beams reinforced with fibers: A state-of-the-art review," *Infrastructures*, vol. 10, no. 3, p. 67, 2025. doi: https://doi.org/10.3390/infrastructures10030067.

[10] H. Kannan, S. K. Veerappan, and M. V. R. Sivasubramanian, "Experimental and numerical investigation of shear performance of RC deep beams strengthened with engineered cementitious composites," *Construction Materials*, vol. 5, no. 3, p. 51, 2025.doi: https://doi.org/10.3390/constrmater5030051.

[11] R. Ali and S. K. Hirde, "Study and review of shear deformation theories for analysis of deep beams," *Current Materials Science*, vol. 18, no. 6, pp. 836–848, 2025. doi: https://doi.org/10.2174/0126661454291237240829103254.

[12] K. Ma, T. Qi, H. Liu, and H. Wang, "Shear behavior of hybrid fiber reinforced concrete deep beams," *Materials*, vol. 11, no. 10, p. 2023, 2018. https://doi.org/10.3390/ma11102023.

[13] R. Kondalraj and G. Appa Rao, "Experimental investigation of RC deep beams with web reinforcement and improvement of ACI 318-19 strut coefficient," Structures, vol. 32, pp. 914–928, 2021. doi: https://doi.org/10.1016/j.istruc.2021.03.052.

[14] A. Ali *et al.*, "Comparative study of shear-span-to-depth and reinforcement ratio on high-strength concrete beams," *Civil and Environmental Engineering*, vol. 21, no. 1, pp. 65-78, 2025.doi: https://doi.org/10.2478/cee-2025-0006.

[15] S. Li, Z. Wu, J. Zhang, and W. Xie, "Experimental study and calculation methods of shear capacity for high-strength reinforced concrete full-scale deep beams," *Materials*, vol. 15, no. 17, p. 6017, 2022. doi: https://doi.org/10.3390/ma15176017.

[16] K. Sogut and B. Ercan, "Behavior of unstrengthened and CFRP-strengthened high-strength concrete deep beams with web openings," *Frontiers in Materials*, vol. 12, Art. no. 1661180, 2025. doi:https://doi.org/10.3389/fmats.2025.1661180.

[17] R. T. S. Mabrouk, M. A. S. Mahmoud, and M. E. Kassem, "Behavior of reinforced concrete deep beams with openings under vertical loads using strut and tie model," *Civil Engineering Journal*, vol. 7, Special Issue, pp. 140–154, 2021. doi: https://doi.org/10.28991/CEJ-SP2021-07-011.

[18] F. Abed, H. El-Chabib, and M. Alhamaydeh, "Shear characteristics of GFRP-reinforced concrete deep beams without web reinforcement," *Journal of Reinforced Plastics and Composites*, vol. 31, no. 16, pp. 1063–1073, 2012. doi: https://doi.org/10.1177/0731684412450350.

[19] A. S. Farghaly and B. Benmokrane, "Shear behavior of FRP-reinforced concrete deep beams without web reinforcement," Journal of Composites for Construction, vol. 17, no. 6, pp. 04013001-1–04013001-10, 2013. doi: https://doi.org/10.1061/(ASCE)CC.1943-5614.0000385.

[20] F. Abed, M. K. Sabbagh, and A. S. Karzad, "Effect of basalt microfibers on the shear response of short concrete beams reinforced with BFRP bars," *Composite Structures*, vol. 269, p. 114029, 2021.doi: https://doi.org/10.1016/j.compstruct.2021.114029.

[21] N. Kachouh, T. El-Maaddawy, H. El-Hassan, and B. El-Ariss, "Shear response of recycled aggregates concrete deep beams containing steel fibers and web openings," *Sustainability*, vol. 14, p. 945, 2022. doi:https://doi.org/10.3390/su14020945.

[22] R. Z. Al-Rousan, "Impact of elevated temperature and anchored grooves on the shear behavior of reinforced concrete beams strengthened with CFRP composites," *Case Studies in Construction Materials*, vol. 14, p. e00487, 2021. doi: https://doi.org/10.1016/j.cscm.2021.e00487.

[23] L. Jin, R. Zhang, L. Li, X. Du, and Y. Yao, "Impact behavior of SFRC beams at elevated temperatures: Experimental and analytical studies," Engineering Structures, vol. 197, p. 109401, 2019. doi: https://doi.org/10.1016/j.engstruct.2019.109401.

[24] A. Rehman, A. Masood, S. Akhtar, S. M. Ibrahim, and M. Shariq, "Experimental and numerical investigation into flexural bond strength of RC beams exposed to elevated temperature," *Construction and Building Materials*, vol. 282, p. 122630, 2021. doi: https://doi.org/10.1016/j.conbuildmat.2021.122630.

[25] S. T. Abdul-Hussain, "Effect of elevated temperatures on compressive and tensile strengths of reactive powder concrete," Journal of Engineering and Sustainable Development, vol. 17, no. 4, pp. 259–278, 2013. [Online]. Available:https://jeasd.uomustansiriyah.edu.iq/index.php/jeasd/article/view/993.

[26] H. Chen, W.-J. Yi, and H.-J. Hwang, "Cracking strut-and-tie model for shear strength evaluation of reinforced concrete deep beams," Engineering Structures, vol. 163, pp. 396–408, 2018. doi: https://doi.org/10.1016/j.engstruct.2018.02.077.

[27] A. F. Deifalla, A. G. Zapris, and C. E. Chalioris, "Multivariable regression strength model for steel fiber-reinforced concrete beams under torsion," *Materials*, vol. 14, no. 14, pp. 1–24, 2021. doi:https://doi.org/10.3390/ma14143889.

[28] K.-H. Tan, G.-H. Cheng, and N. Zhang, "Experiment to mitigate size effect on deep beams," Magazine of Concrete Research, vol. 60, no. 10, pp. 709–723, 2008. doi: https://doi.org/10.1680/macr.2007.00030.

[29] Iraqi Specification No. 5/2019, "Portland Cement," Central Organization for Standardization and Quality Control (COSQC), Baghdad, Iraq, 2019.

[30] Iraqi Specification No. 45/1984, *"Aggregate from Natural Sources for Concrete and Construction,"* COSQC, Baghdad, Iraq, 1984.

[31] BS EN 12390-3:2019, "Testing Hardened Concrete—Part 3: Compressive Strength of Test Specimens," London, U.K.: British Standards Institution, 2019.

[32] ASTM C39/C39M-21, "Standard Test Method for Compressive Strength of Cylindrical Concrete Specimens," West Conshohocken, PA, USA: ASTM International, 2021.

[33] A. A. Asghari, Z. Tabrizian, M. H. Beygi, G. G. Amiri, and B. Navayineya, "An experimental study on shear strengthening of RC lightweight deep beams using CFRP," Journal of Rehabilitation in Civil Engineering, vol. 2, no. 2, pp. 9–19, 2014. doi: https://doi.org/10.22075/JRCE.2014.204.

[34] Y. Xu, Y. L. Wong, C. S. Poon, and M. Anson, "Influence of PFA on cracking of concrete and cement paste after exposure to high temperatures," *Cement and Concrete Research*, vol. 33, no. 12, pp. 2009–2016, 2003. doi: https://doi.org/10.1016/S0008-8846(03)00216-3.

[35] Z. Zhang, D. Zhang, J. Zhou, D. Zhang, and K. H. Tan, "A critical review on high temperature performance of sustainable cementitious material," *Materials Sustainability*, vol. 3, p. 39, 2025. doi: https://doi.org/10.1038/s44296-025-00081-9.

[36] A. M. Neville, Properties of Concrete, 4th ed. Harlow, U.K.: Pearson Education Limited, 2011.